Histone H2AX Y142 phosphorylation is a low abundance modification

Article (Accepted Version)

Histone H2AX Y142 phosphorylation is a low abundance modification

Abubakar A. Hatimy[1], Martin J. G. Browne[2], Andrew Flaus[2], Steve M. M. Sweet[1].
1: Genome Damage and Stability Centre, University of Sussex, Brighton, UK.
2: Centre for Chromosome Biology, School of Natural Sciences, National University of Ireland, Galway, Ireland.
Correspondence: Dr Steve Sweet, s.m.sweet@sussex.ac.uk

Keywords: chromatin; histone; phosphorylation; DNA damage; selected reaction monitoring.

Abstract

We employ targeted mass spectrometry to compare the levels of H2AX S139 phosphorylation (γH2AX) and Y142 phosphorylation. We use synthetic peptides to facilitate MS optimization and estimate relative detection efficiencies for the different modifications. Despite phosphopeptide enrichment from large amounts of starting material, we are unable to detect endogenous H2AX Y142 phosphorylation, indicating that it is present at low abundance (<1%). We also calculate the relative levels of H2AX compared to other H2A isoforms and quantify the proportion of H2AX that is phosphorylated on S139 (γH2AX) after ionizing radiation.

Introduction

S139 phosphorylation

The histone H2A family variant, H2AX, is distinguished from canonical H2A family members through a 22 amino acid C-terminal tail [1]. Phosphorylation of the C-terminal domain of H2AX at position 139 (γH2AX) is a rapid response to DNA double-strand breaks (DSB). S139 is phosphorylated by ATM, ATR and DNA-PK, which are phosphatidylinositol 3-kinase-related kinases. γH2AX foci are widely used as diagnostic markers of DSB. The utility of γH2AX as a marker stems from the rapid (<1 min) and extensive nature of this modification. Rogakou *et al.* observed that approximately 1% of total H2AX becomes phosphorylated per gray of ionizing radiation (IR), and extrapolated from H2AX relative abundance that each DSB results in γH2AX covering on average 2 million bp [2]. The biological function of such large γH2AX domains is not clear, and the H2AX histone is not essential for DSB repair, however $H2AX^{-/-}$ mice show increased ionizing radiation sensitivity, as well as increases in chromatid breaks and dicentric chromosomes [3].

Y142 phosphorylation

The H2AX C-terminal domain can also be phosphorylated on tyrosine 142 by the WSTF remodelling factor kinase [4-6]. Cook *et al.* show that dephosphorylation of Y142 upon DNA damage avoids apoptosis. Using synthetic phosphopeptides, they demonstrate binding of pro-apoptotic factors to S139 Y142 doubly-phosphorylated peptides: the implication is that Y142 phosphorylation is abundant, and will be located in proximity to DNA damage. While kinases and phosphatases responsible for creating and removing this modification have been identified, the basal level of Y142 phosphorylation

is unknown, although our earlier intact histone MS analysis indicates that in HeLa cells it is not greater than ~10% [7]. Scully *et al.* expressed epitope-tagged H2AX in $H2AX^{-/-}$ mouse ES cells and identified a number of H2AX modifications by mass spectrometry, including S139 and T101 phosphorylation, however Y142 phosphorylation was not detected [8]. The role of Y142ph in the DNA damage response is of great interest, with the identification of putative interacting proteins that recognise the doubly phosphorylated C-terminal tail [9]. Mutation of these residues has been carried out in the chicken DT40 cell line and revealed that Y142A IR sensitivity is rescued by co-mutation of S139A [10].

H2AX levels across cell lines and in the genome

Given the role of H2AX phosphorylation in signalling DNA damage and recruiting repair proteins, it is interesting to consider the levels of H2AX present across the genome in human cells. Rogakou *et al.* employed two-dimensional gel separation of histone preparations with Coomassie staining to quantify H2AX as a proportion of all H2A1, H2A2 and H2AX signal. They analysed four human cell lines and found H2AX makes up 2-25% of the total [2].

Materials and methods

Synthetic peptides and recombinant histones

Peptides listed below were synthesized by JPT (Germany).

Synthetic Peptide Sequence		
GHYAERATQASQEY	KGHYAERGKTGGKAR	GKTGGKARAKAKSR
GHYAERATQA-pS-QEY	KGNYAERGKTGGKAR	GKQGGKARAKAKSR
GHYAERATQASQE-pY-		

Recombinant H2AX and H2A1B were expressed in *E. coli* Rosetta 2(DE3) pLysS. Cultures were incubated at 37°C with 180 rpm agitation. Unlabelled proteins were grown in 2YT media to OD_{600} 0.6 and induced with isopropyl-β-D-thiogalactoside (IPTG) for 4 h before harvest. ^{15}N-labelled proteins were produced using a two-step expression procedure. 2YT cultures were grown to OD_{600} 0.6 and cells collected by centrifugation. Cells were gently resuspended in an equivalent volume of pre-warmed minimal media (50 mM Na_2HPO_4, 50 mM KH_2PO_4, 1 g/L $(^{15}NH_4)_2SO_4$, 2 mM $MgSO_4$, 20 mM citric acid, 30 mg/L thiamine, pH7.0) and incubated at 37°C for 30 min prior to IPTG induction for 4 h and harvest. Recombinant histones were purified according to the established inclusion body wash procedure followed by cation exchange chromatography [11]. Purified histones were dialysed into water and lyophilised for long term storage. The recombinant proteins were resuspended in water at a concentration of 2 mg/ml, based on absorbance at 278 nm using extinction coefficients 5960 and 4470 $M^{-1}cm^{-1}$ for H2AX and H2A1B, respectively. MS analysis of ^{15}N H2AX indicated that labelling was >98% complete. Recombinant histone sequences are shown below. Synthetic peptide sequences are underlined.

H2AX:
MSGRGKTGGKARAKAKSRSSRAGLQFPVGRVHRLLRKGHYAERVGAGAPVYLAAVLEYLTAEILELAGNAARDNK
KTRIIPRHLQLAIRNDEELNKLLGGVTIAQGGVLPNIQAVLLPKKTSATVGPKAPSGGKKATQASQEY

H2A1B:
MSGRGKQGGKARAKAKTRSSRAGLQFPVGRVHRLLRKGNYSERVGAGAPVYLAAVLEYLTAEILELAGNAARDNK
KTRIIPRHLQLAIRNDEELNKLLGRVTIAQGGVLPNIQAVLLPKKTESHHKAKGK

Cell lines and cell culture: Human U2-OS and HeLa cells were cultured in Dulbecco's modified Eagle's medium (DMEM) supplemented with 10% foetal calf serum, 2mM L-glutamine, 100 U/ml penicillin, and 100 µg/ml streptomycin. Epstein Barr virus-transformed wild-type lymphoblastoid cells (LCLs; a gift from Mark O'Driscoll; [12]) were cultured in Roswell Park Memorial Institute (RPMI) 1640 medium supplemented with 15% foetal calf serum, 2mM L-glutamine, 100 U/ml penicillin, and 100 µg/ml streptomycin. Approximately $6x10^7$ cells were grown for each sample.

Irradiating Cells: U2-OS cells were irradiated with a dosage of 20 Gy using a ^{137}Cs source. Cells were immediately placed in a 37°C incubator and were left to recover for either 5 minutes, 30 minutes, or 60 minutes. Upon recovery, cells were spun down and were immediately flash frozen and stored at -80°C before sample preparation.

Nuclei Isolation and Acid Extraction: Nuclei Isolation Buffer 250 (NIB-250) was prepared: 15 mM Tris HCl (pH 7.5), 60 mM KCl, 15 mM NaCl, 5 mM $MgCl_2$, 1 mM $CaCl_2$, and 250 mM Sucrose. NIB-250 was supplemented with the following phosphatase and protease inhibitors: 10 mM Na-butyrate, 0.5 mM AEBSF, 2 µM leupeptin, 1 µM Pepstatin A, 1 µM aprotonin, 2 mM PMSF, 50 mM NaF, 2 mM Na-orthovanadate, and 60 mM β-glycerophosphate. NIB-250 with 0.3% NP-40 was added to the cells at a ratio of 10:1. Cells were incubated on ice for 5 min and then subsequently spun down at 600 rcf for five min at 4°C. The supernatant was discarded and then NIB-250 without NP-40 was added to the cell pellet and spun down again, twice. The remaining pellet consisted of isolated nuclei. The isolated nuclei was vortexed slowly and 0.4N sulphuric acid was added to the cells at a final ratio of 5:1. The nuclei-H_2SO_4 suspension was left to incubate on ice for 60 minutes and then spun down at the centrifuge's maximum speed for 5 minutes at 4°C. The supernatant was transferred to a microcentrifuge tube. To the supernatant, 100% trichloroacetic acid (TCA) was added to give a final concentration of 20% TCA. The mixture was left to precipitate overnight at 4°C. The precipitate was then spun down at the microcentrifuge's maximum speed. The pellet was resuspended in chilled acetone with 0.1% hydrochloric acid. The sample was then spun down, washed twice with acetone, left to air dry, and finally dissolved in water.

Derivitisation and Trypsinisation: A modified version of the derivatization protocol described in Maile *et al.* was employed [13]. From the acid extracted histone sample, 5 µg was used to make up a volume of 9 µl. 1 µL of 1M tetraethylammonium bromide (TEAB) was added to the sample to buffer the subsequent reaction. 1 µL of diluted propionic anhydride (in water to a ratio of 1:100) was added to the histones. The samples were vortexed for 2 minutes at room temperature. To quench the derivitisation reaction, 1 µL of 80 mM hydroxylamine was added and the samples were left to incubate for 20 minutes at room temperature. The pH of the samples was measured to ensure optimal trypsin digestion, ~pH8.5. 250 ng of trypsin was added to each sample and left to digest at 37°C for 4 hours or overnight. Upon digestion, a second round of derivitisation was carried by adding 3 µL of 1:100 diluted propionic anhydride. The samples were vortexed for 2 minutes at room temperature. 3 µL of 80 mM hydroxylamine was then added to quench the second round of derivitisation.

Phosphopeptide enrichment: TiO_2 metal oxide affinity chromatography was approximately as described in Matheron *et al.* [14]. Briefly, TiO_2 beads (Titansphere; 5 µm; GL Sciences, Japan) were resuspended at 10 mg/ml in 30% acetonitrile (ACN), 0.1% TFA. 50 µL of this slurry was packed by centrifugation (400*g*) into a GELoader tip spin column (Eppendorf; 0.5-20 µL volume) fritted with a C8 filter membrane (Empore). The spin column was equilibrated with loading buffer (80% ACN, 6% TFA; 50 µl at 2,200), the sample was loaded (2 x 50 µL; 200*g*) and the column washed twice (50 µL; 50% ACN, 0.5% TFA, 0.2 M NaCl; 500*g*), with salt omitted in the second wash. Phosphopeptides were eluted with 20 µL of 10% NH_4OH (200*g*), into 25 µL 10% FA. A final elution of 3 µL 80% ACN, 2% FA was employed to release peptides from the C8 frit. Further acid (3 µL FA) was added to the eluates. Eluates were dried in a vacuum centrifuge and resuspended in 10 µL 0.1% TFA.

Nano-LC/MS: Peptide samples were analyzed by nano-LC-MS (ThermoFisher U3000 nanoLC and Orbitrap XL mass spectrometer). Peptides were loaded onto a C18 trapping cartridge (Pepmap100 C18; 0.3 x 5 mm i.d.; 5 µm particle size) for 5 min at a flow-rate of 5 µL/min in 0.1% TFA loading buffer. Peptides were separated on an analytical column (PepMap100; 25 cm x 75 µm; 5 µm particle size) by a gradient from 1 to 35% ACN over 28 min, in the presence of 0.1% FA, at a flow rate of 0.3 µL/min.

Time	0	15	25	28	28	35	35
% acetonitrile	1	12	35	60	90	90	1

Nanospray was from a New Objective emitter with 10 µm tip (FS360-20-10-N-20). Pseudo-SRM was carried out in the linear ion trap of an Orbitrap XL, with a precursor isolation window of 2 m/z, an ion-trap fill time of maximum 50 ms and an LTQ target ion count of 1E4 [15]. A high-resolution precursor scan was carried out in the Orbitrap (5E5 target). Total cycle time was <30 s, enabling sufficient points across eluting peptide peaks for quantitation. For the TiO2-enrichment eluates, in addition to the targeted LTQ events, a data-dependent event was included, to enable identification of untargeted enriched phosphopeptides.

Pseudo-SRM creation and analysis: Skyline v3.1 (MacCoss Lab, University of Washington) was used for both development of pseudo SRM methods and for data analysis [16]. Peptide sequences for protein of interest were obtained from Uniprot and entered into Skyline. Putative and known post-translational modifications of interest were added to the peptides. Predicted b and y ions were surveyed on the instrument. To distinguish between different isobaric masses at least three transitions were selected that were unique to each peptide. Transitions used for data analysis are listed in **Supplementary Table 1**.

Data analysis

Database searching for the TiO_2-enriched samples employed Mascot and the Swissprot database. Settings were as follows: two missed cleavages; precursor 5 ppm error; fragment 0.6 Da error; variable modifications of acetylation (K), mono-, di- and trimethylation (K), phosphorylation with neutral loss (S,T), phosphorylation (Y). Three U2-OS acid extract TiO_2 eluates (25 µg, 50 µg, 50 µg + Y142ph peptide) were run as a combined search. Mascot results were filtered to require expectation value <0.05 and bold red and exported as .csv. The peptide list was sorted according to descending E-value and duplicate pep_scan_titles were removed. 1393 peptide identifications remained. Duplicates in all three of pep_seq and pep_var_mod and pep_var_mod_pos were removed (again removing lowest E-value duplicates). 456 identifications remained. 307 of these were phosphorylated (including spiked Y142ph peptide). Some were clearly false-positives (as expected given E-value 0.05): filtering to require E-value <0.01 leaves 370 identifications, of which 230 were phosphorylated.

Results

In order to develop sensitive selected reaction monitoring (SRM) assays for H2AX phosphopeptide detection by mass spectrometry, as employed previously for histone H3 methylation analysis [17], we designed synthetic peptides containing either phosphorylated Y142, phosphorylated S139 or no modification. To allow determination of relative ionization efficiency, these peptides were synthesized concatenated with a common quantification peptide. After trypsin digestion to separate the two peptides, the released phosphopeptides were fragmented (**Figure 1a**), and the indicated fragments were quantified in pseudo-SRM assays utilising the linear ion trap of an Orbtrap XL [15]. The H2AX C-terminal peptides were detected in both singly- and doubly-charged forms. The singly-charged species was preferred for sensitive detection of low levels of C-terminal peptide in the presence of abundant canonical histone peptides, due to low background in this m/z region for these transitions. The released H2AX-specific quantification peptide (GHYAER) acts as an internal standard: the ionization efficiency of the C-terminal peptide is measured relative to the quantification peptide in each case (**Figure 1b**). We found that the phosphorylated peptides were detected 2.6x and 8.3x less well than the unphosphorylated peptide (S139ph and Y142ph, respectively; **Figure 1b**).

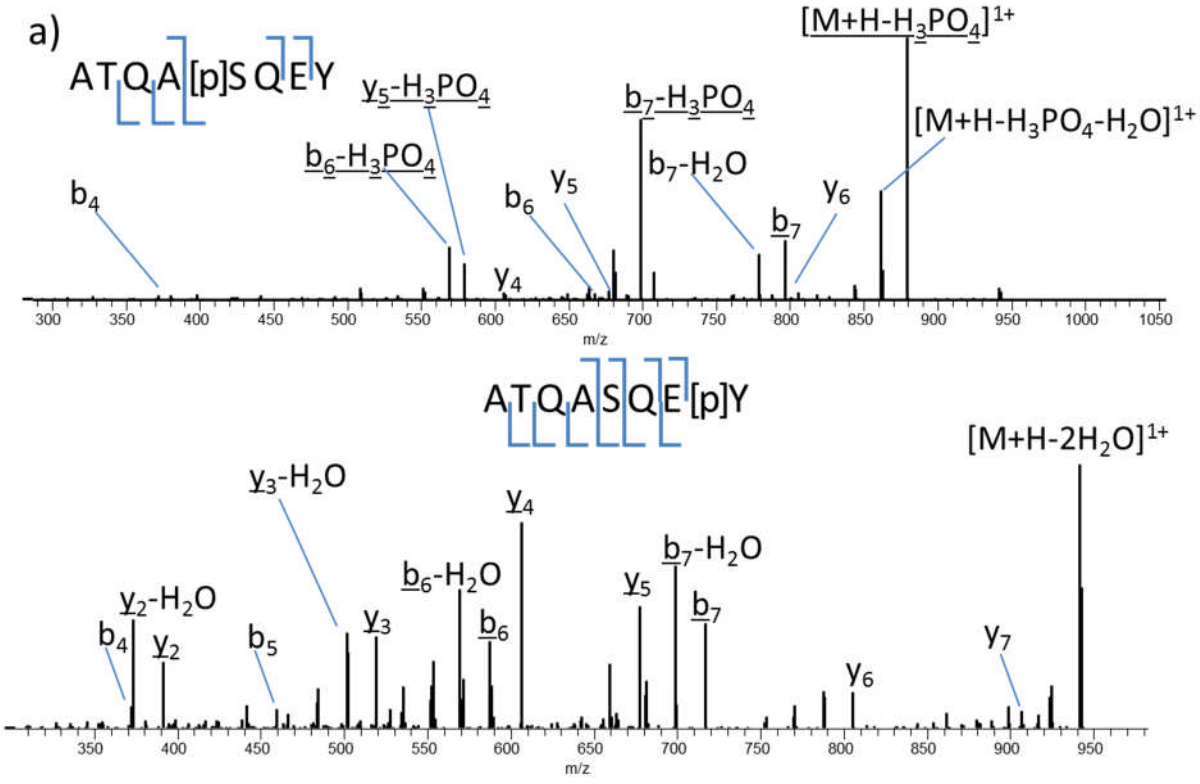

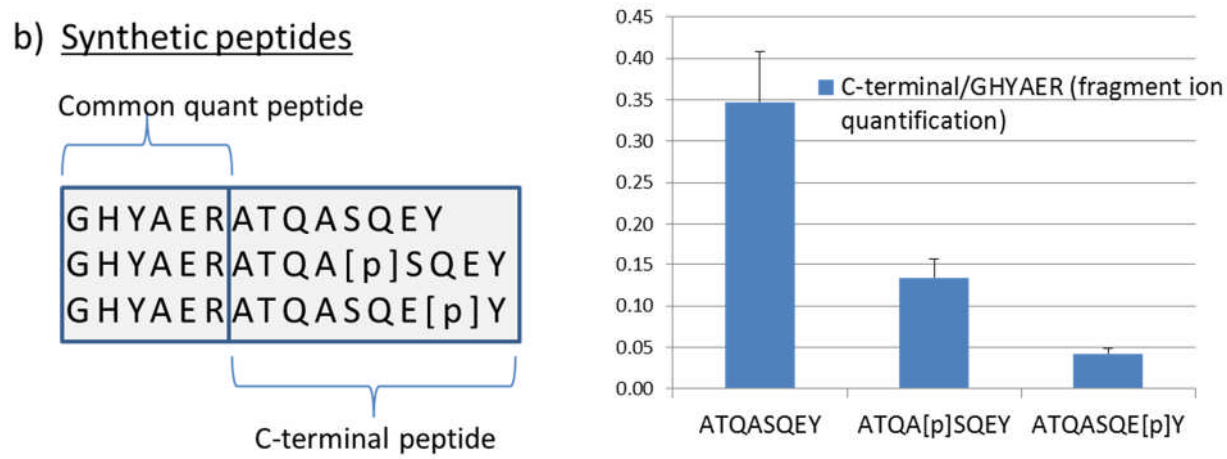

Figure 1. a) MS/MS fragmentation of singly-charged ATQASQEY S139 or Y142 phosphorylated precursors. Fragment ions used for quantitation are underlined. b) Concatenated synthetic peptides allow assessment of relative detection efficiency after trypsin digestion, nanoLC separation and pseudo-SRM peptide fragmentation. Both N-terminal and C-terminal peptides are unique to H2AX. Error bars show standard deviation (n=3).

We apply this correction factor to data obtained from U2-OS cells after ionizing radiation (IR) to estimate that approximately 75% of H2AX in the sample was phosphorylated at S139 60 minutes after 20 Gy IR (**Figure 2**).

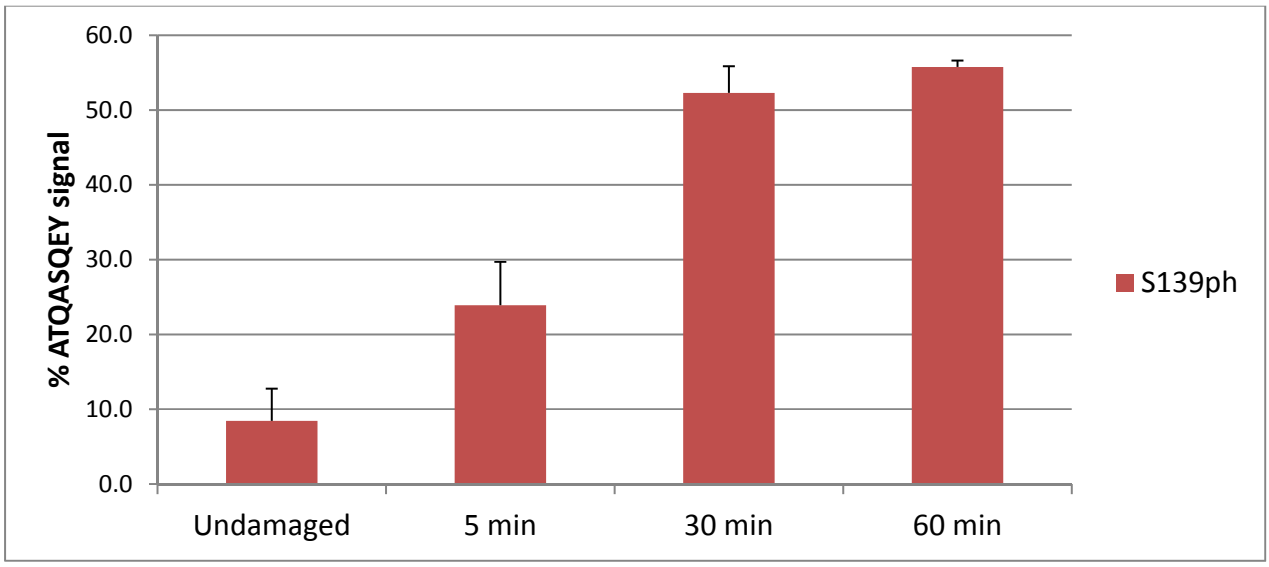

Figure 2. Quantification of γH2AX Ser139 phosphorylation after DNA damage. A) Time-course after 20 Gy IR (U2-OS). Fragment ions from the singly-charge unmodified and S139 phosphorylated precursors were quantified. Mean of two biological replicates is shown, each of which was analysed in technical triplicate. Error bars show standard deviation. Data shown is uncorrected for detection efficiency.

Y142 phosphorylation

We did not detect Y142ph in undamaged cells or any of the time-points shown in Figure 2. We considered that the failure to detect Y142 phosphorylation in our histone preparations could indicate that this modification is present only at low abundance, given that we were able to detect the synthetic Y142ph peptide with reasonable sensitivity. We therefore carried out a TiO_2 metal oxide affinity phosphopeptide enrichment step on a histone preparation from undamaged U2-OS cells, which we had shown to contain only low levels of γH2AX phosphorylation (approximately 4%). We carried out a parallel enrichment on a control sample, containing 50 pmol BSA and 0.5 pmol of α-casein, Y142ph, S139ph and unmodified synthetic peptides (**Figure 3**). We see efficient enrichment of Y142ph, S139ph from the control sample, in addition to the expected α-casein phosphopeptides. We also see efficient enrichment of S139ph from the undamaged U2-OS sample, alongside a number of other phosphopeptides from other histones and low-level phosphoproteins present in the acid-extract. However no Y142ph signal was detected from the U2-OS sample.

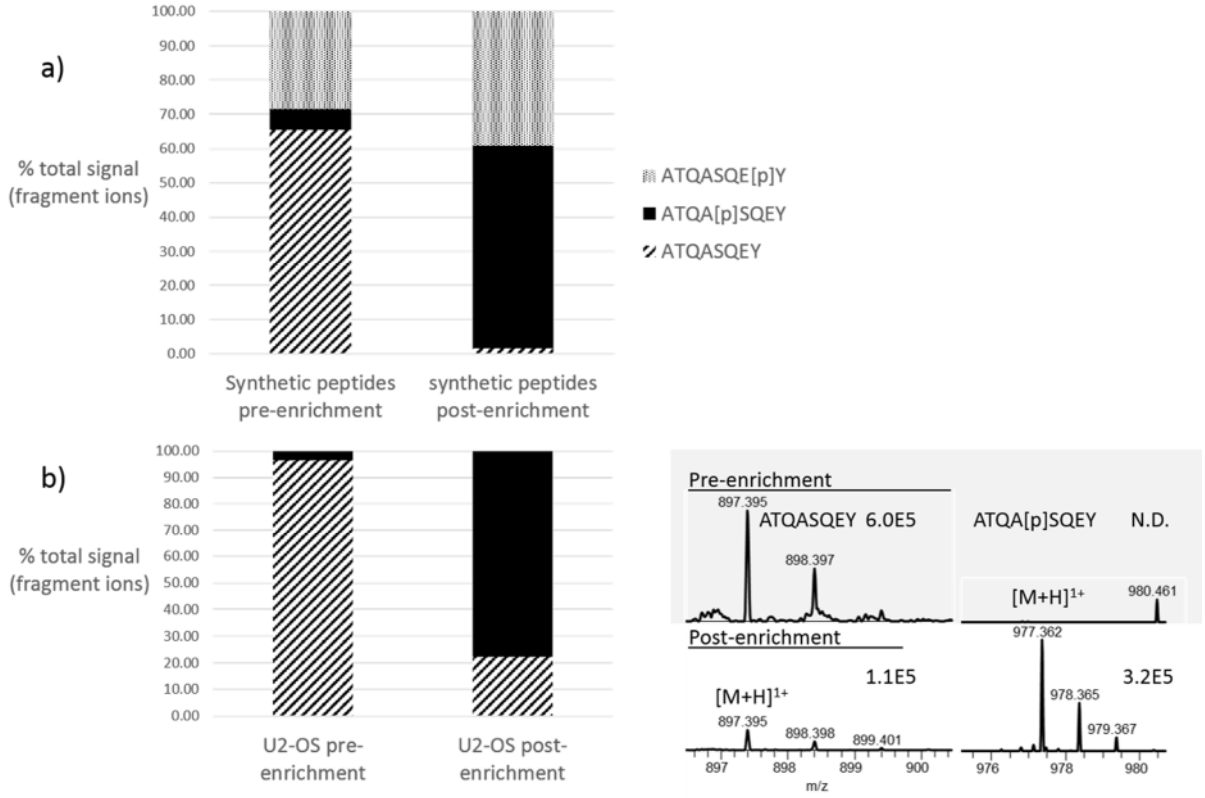

Figure 3. TiO_2-based phosphopeptide enrichment of H2AX C-terminal peptides. A) Successful enrichment of S139ph and Y142ph peptides from 100x excess BSA peptides B) Enrichment of endogenous S139ph peptide from undamaged U2-OS, relative to the unmodified peptide. LHS: quantification of fragment ions from singly-charged precursors. RHS: precursor ions (with relative intensity shown).

To further verify that there was no technical problem with our enrichment, we spiked Y142ph peptide (2 pmol) into a U2-OS sample (50 μg acid extract). Enrichment from the spiked sample was carried out in parallel with enrichment from an equivalent unspiked sample. As before, endogenous S139ph was enriched in both cases. Y142ph was successfully enriched from the spiked sample, but not detectable

in the unspiked sample (**Figure 4**). Although the U2-OS acid extracts contain mainly histones, TiO_2 enrichment allowed identification of 232 distinct phosphopeptides (with an expectation value <0.01), mainly from low abundance non-histone proteins (**Supp. table 2**). These identifications included the previously described CDK3 Y15 tyrosine phosphorylation. In addition to H2AX S139ph, previously reported core histone phosphorylations H3 S10ph, S57ph and H4 S47ph were also identified, as well as nine H1 sites.

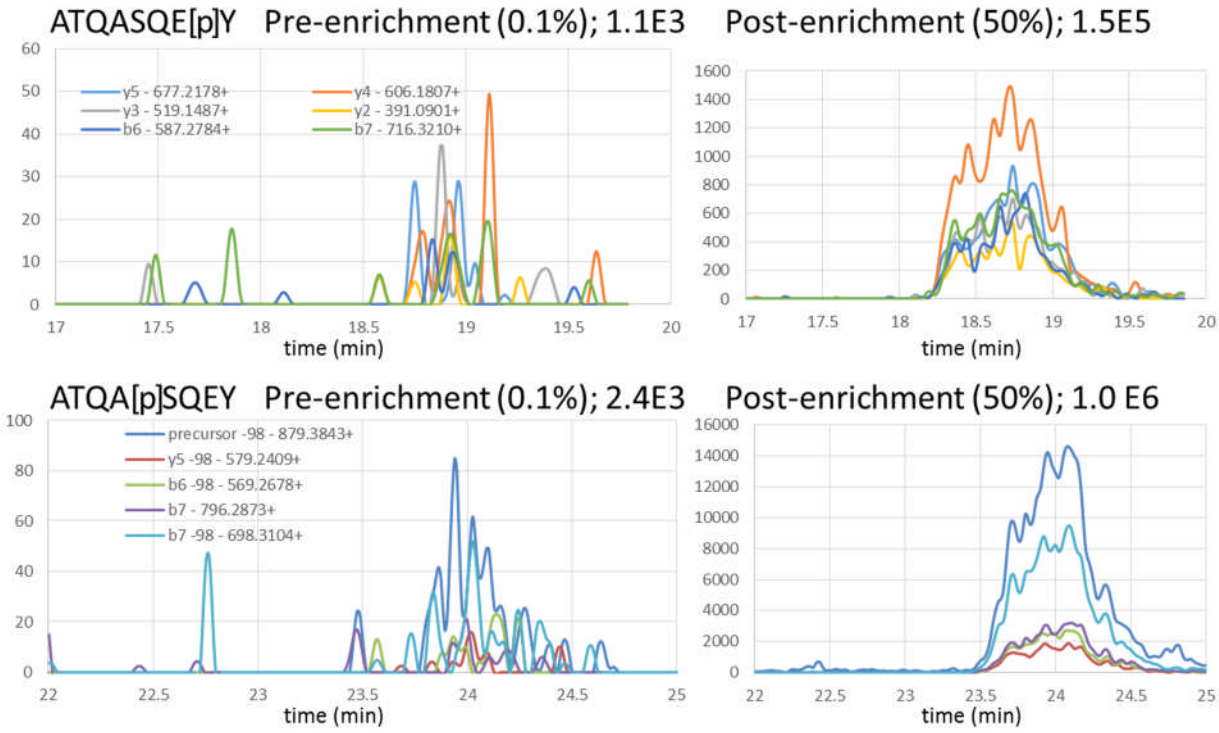

Figure 4. Successful enrichment of Y142ph synthetic peptide spiked into U2-OS acid extract. 0.1% of the 50 µg sample was analysed pre-enrichment; both Y142ph (synthetic) and S139ph are barely detectable using pseudo-SRM (precursor ions are not detectable; data not shown). After enrichment both H2AX phosphopeptides are detected with good signal-to-noise.

H2AX abundance across cell lines

We compared the abundance of two peptides unique to H2AX (GKTGGKAR and KGHYAER) to similar peptides in other H2A family members in three cell lines: U2-OS, HeLa and an EBV-transformed lymphoblastoid cell line (LCL; **Table 1**). In this analysis we employed a propionylation derivatization step prior to, and after, trypsin digestion. In order to control for possible variations between sample preparations, ^{15}N-labelled recombinant H2AX and H2A1B were spiked into the three samples. These samples were then derivatized and digested as normal and analysed in technical triplicate. **Figure 5** shows the normalized ratio of endogenous H2AX to ^{15}N H2AX peptide for each cell line, indicating U2-OS contains the highest relative abundance of H2AX, >2x more than HeLa. The two H2AX peptides both give similar results.

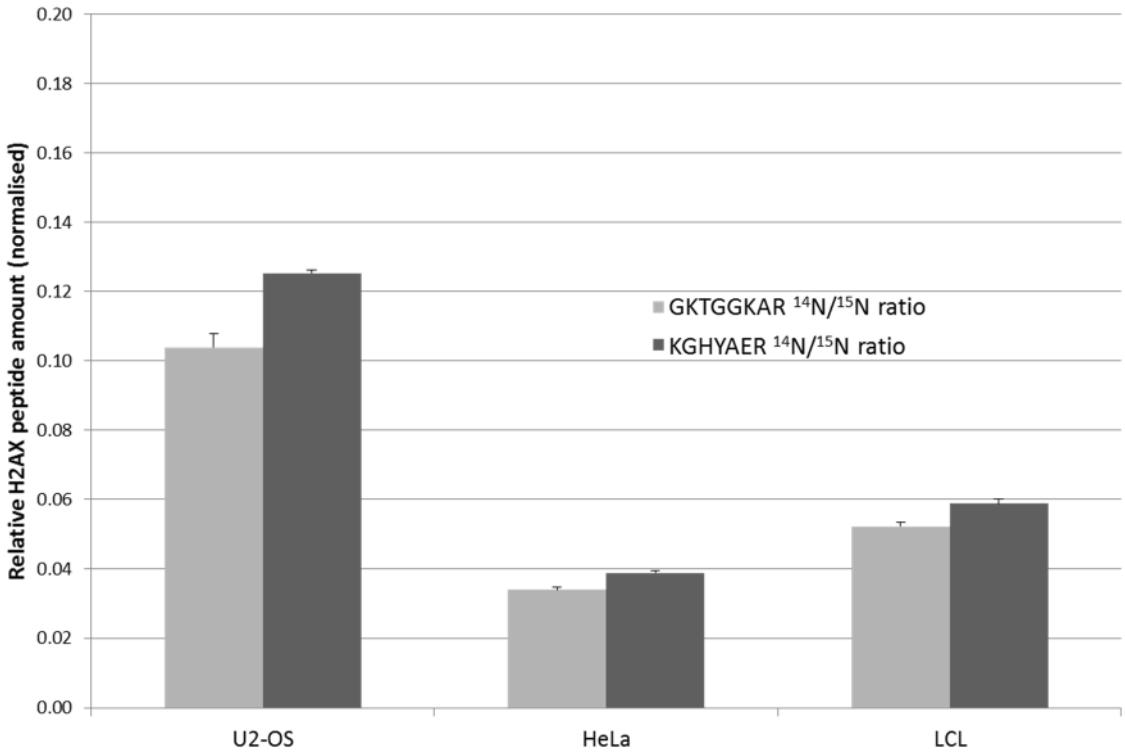

Figure 5. **Relative amount of H2AX across three cell lines.** ^{15}N recombinant H2AX and H2A1B were spiked into U2-OS, HeLa and LCL extracts; ratios for diagnostic peptides were calculated and normalised to ratio of H2A1B GKQGGKAR, to control for small differences in starting acid extract amounts. Error bars show standard deviation.

H2AX abundance compared to other H2A family variants

We quantified the signal from the two peptides unique to H2AX as a proportion of the signal from closely related H2A family peptides (**Figure 6** and **Table 1**). Concatenated peptides were again employed to correct for detection efficiencies, as above. The same trend with respect to H2AX abundance across the three cell lines is observed, as expected (U2-OS>LCL>HeLa). The estimates of H2AX abundance are not identical for the two different H2AX peptides. The proportion of H2AX calculated from the KGHYAER peptide is consistently higher than that calculated from the GKTGGKAR peptide, This difference may be due to the different ionization properties of the non-canonical peptides (KGNYSER and GKQGGKVR), synthetic versions of which were not available for correction. Importantly, both peptides give a highly similar relative abundance across the three cell lines. The values shown in Table 1 represent upper estimates, as four divergent H2A variants are not measured at all.

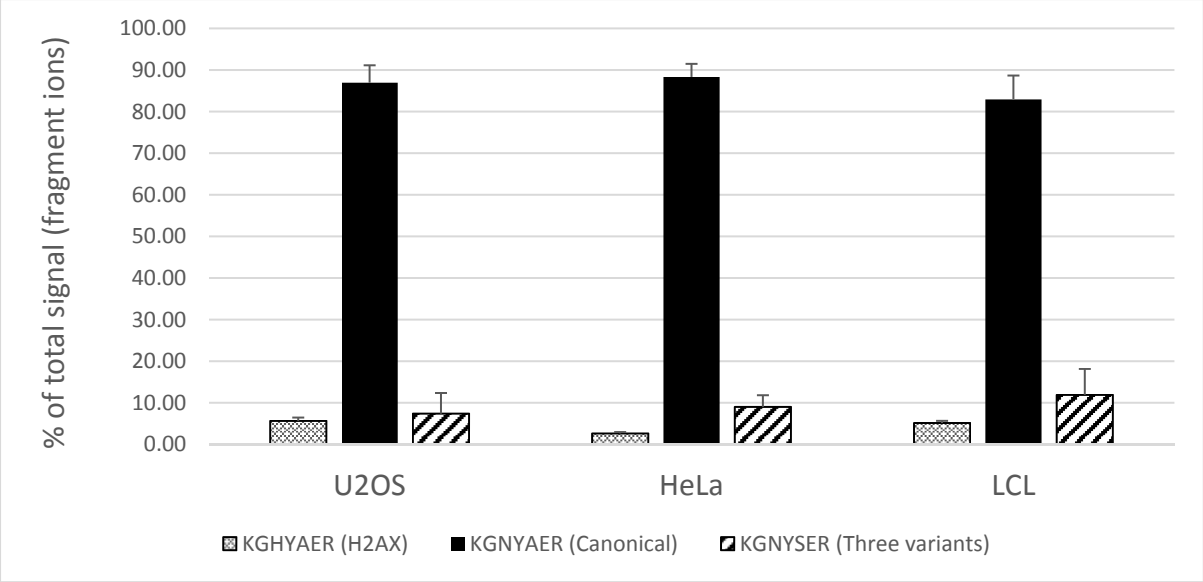

Figure 6. Quantification of H2AX abundance relative to other H2A isoforms. Relative H2AX levels (corrected for detection efficiency) from U2-OS, HeLa and LCL. Quantification is of fragment ions from doubly-charged precursors. Data is from two biological replicates, analysed in technical triplicate. KGHYAER is unique to H2AX; KGNYSER is unique to H2A 1B, 1D and 3. Error bars show standard deviation.

Measured peptide	Protein(s)	U2OS	HeLa	LCL
GKTGGKAR	H2AX	4 (0.7)	1 (0.6)	2 (0.03)
GKQGGKAR	11 H2A (1A, 1B, 1C, 1H, 1J, 1D, 1, 2A, 2C, 3, 2B)	96 (0.6)	98 (0.9)	98 (0.2)
GKQGGKVR	H2AJ	1 (0.05)	1 (0.3)	0 (0.1)
not measured	H2AB1, H2AB2, H2AV, H2AZ	n.m.	n.m.	n.m.
Total	**17**	**100**	**100**	**100**
KGHYAER	H2AX	6 (0.8)	3 (0.3)	5 (0.5)
KGNYAER	9 H2A (1A, 1C, 1H, 1J, 1, 2A, 2C, 2B, J)	87 (4.2)	88 (3.1)	83 (5.7)
KGNYSER	H2A 1B, 1D, 3	7 (5.0)	9 (2.8)	12 (6.2)
not measured	H2AB1, H2AB2, H2AV, H2AZ	n.m.	n.m.	n.m.
Total	**17**	**100**	**100**	**100**
	H2AX average	5	2	4

Table 1. H2AX abundance relative to H2A family members. GKTGGKAR was found to be detected 1.1x better than the canonical version, GKQGGKAR. The H2AX peptide KGHYAER was detected 1.7x better than the canonical version KGNYAER. The proportions are corrected accordingly in the table above. Data is from two biological replicates, analysed in technical triplicate. The standard deviation is shown in brackets.

Discussion

We have developed pseudo-SRM assays to quantify levels of H2AX C-terminal phosphorylation. The C-terminal phosphopeptides of H2AX are not the most straight-forward peptides to analyse in positive-mode mass spectrometry, being without basic residues to balance the negative charge of the phosphate group. Nonetheless, both S139ph and Y142ph peptides ionize to give doubly- and singly-charged species, which can be fragmented to give diagnostic fragment ions. The two phosphopeptides show considerable difference in retention time, avoiding co-fragmentation of the isobaric species. We detect variable levels of γH2AX (S139ph) from undamaged U2-OS (4% and 12% in the two biological replicates contributing to Figure 2), increasing to 75% 1 h after 20 Gy IR and correction for detection efficiency. We note that this level of S139ph is substantially higher than that previously reported by Rogakou *et al.* (30-50%), albeit using a different method and for different cell lines [2]. Our correction factor controls for ionization efficiency and fragmentation efficiency of the unmodified and phosphorylated peptides, however it does not control for differences in trypsin release of the measured peptides. We consider it possible that phosphorylation of S139 may affect the ability of trypsin to cleave the proximal lysine, producing the quantified fully tryptic peptide: a set of synthetic peptides incorporating the endogenous trypsin cleavage site would enable this to be tested (APSGGKKATQASQEY). The 75% estimate should therefore be treated with caution.

We were unable to detect endogenous H2AX Y142ph, even after enrichment of phosphopeptides from large amounts of histone preparations (50 µg). Notably, synthetic Y142ph was detected and enriched without difficulty. Given that after enrichment we identify endogenous S139ph from undamaged cells (approximately 5% abundance) with a signal to noise ratio of over 100, we should be able to identify S139ph at 20-40x lower abundance, i.e. 0.25-0.125% abundance within the genome. Our synthetic peptide data indicates that the Y142ph peptide is detected 3.2 x less well than the S139ph peptide, implying a conservative detection level of 0.8% overall abundance. Large-scale phosphoproteomic studies have similarly failed to detect Y142ph, even when S139 phosphorylation was detected, and in the absence of DNA damage treatments [18, 19]. We conclude that the stoichiometry of Y142ph is low, at least below 1% of H2AX in undamaged U2-OS. Of the early papers describing H2AX Y142ph, Krishnan *et al.* also used U2-OS cells [6]. It is possible that Y142ph levels are higher in the other cell lines studied previously (HEK 293T, mouse 3T3 and mouse embryonic fibroblasts). However if Y142 phosphorylation plays a significant physiological role in apoptosis and the DNA damage response, it seems unlikely to vary dramatically across cell lines or between human and mouse.

This low stoichiometry has implications for the use of Y142ph antibodies: Xiao *et al.* raised an antibody that appears to strongly prefer Y142ph, but nevertheless still binds unphosphorylated Y142 (ELISA Xiao *et al.* Supp. Fig. 1). With >100:1 ratio of unmodified to Y142ph, this background could be problematic [4]. The low abundance of Y142ph also has implications for models involving binding of proteins to both S139ph and Y142ph simultaneously [5, 9]: co-localisation of S139ph and Y142ph on the same H2AX C-terminal tail would be most likely to occur at extremely high levels of DNA damage, when the majority of H2AX S139 is phosphorylated. Analysis of the role of Y142 through site-directed mutagenesis [10] is complicated by the observation that Y142 mutation interferes with binding of proteins such as MDC1 to γH2AX [20].

Removal of WSTF, the kinase responsible for Y142 phosphorylation, reduces γH2AX formation and abrogates the DNA damage response, however it is unclear if this is related to H2AX Y142 phosphorylation or to the chromatin remodelling role of this factor [4]. Our results would be consistent with an indirect effect.

We analyse H2AX abundance in three cell lines, and find that H2AX constitutes between 2-5% of the thirteen H2A family members quantified: the total level would therefore be lower when the remaining four, more divergent, variants are taken into account (H2AV, H2AZ, H2AB1, H2AB2). This level seems reasonable, considering that the gene encoding H2AX, H2AFX, is one of 24 H2A family (H2AF) genes, encoding 17 unique H2A isoforms (Uniprot curated protein family). Therefore if all expression levels were even, H2AX would make up 4.2% of cellular H2A.

Our estimate for HeLa of 1.8% H2AX is very similar to that of Rogakou *et al.* (2.4%) [2]. Presumably the divergent H2A family members do not co-migrate with the canonical H2As upon two-dimensional gel electrophoresis, and therefore were also not quantified by Rogakou *et al*.

Acknowledgements and funding

Dr Rita Colnaghi and Professor Mark O'Driscoll for advice and the generous gift of the LCL cells. Dr Lisa Woodbine for advice on cell culture. Dr Stuart Rulten for advice and assistance with IR treatment. Dr Shabaz Mohammed (University of Oxford) for advice on phosphopeptide enrichment. AH is funded by a School of Life Sciences PhD studentship, SMMS is funded by an MRC career development award.

[1] Pinto, D. and A. Flaus, *Structure and Function of Histone H2AX*, in *Genome Stability and Human Diseases*, H.-P. Nasheuer, Editor 2010, Springer Netherlands. p. 55-78.

[2] Rogakou, E.P., D.R. Pilch, A.H. Orr, V.S. Ivanova, et al., DNA Double-stranded Breaks Induce Histone H2AX Phosphorylation on Serine 139. *Journal of Biological Chemistry* 1998, *273*, 5858-5868.

[3] Celeste, A., S. Petersen, P.J. Romanienko, O. Fernandez-Capetillo, et al., Genomic Instability in Mice Lacking Histone H2AX. *Science* 2002, *296*, 922-927.

[4] Xiao, A., H. Li, D. Shechter, S.H. Ahn, et al., WSTF regulates the H2A.X DNA damage response via a novel tyrosine kinase activity. *Nature* 2009, *457*, 57-62.

[5] Cook, P.J., B.G. Ju, F. Telese, X. Wang, et al., Tyrosine dephosphorylation of H2AX modulates apoptosis and survival decisions. *Nature* 2009, *458*, 591-596.

[6] Krishnan, N., D.G. Jeong, S.-K. Jung, S.E. Ryu, et al., Dephosphorylation of the C-terminal Tyrosyl Residue of the DNA Damage-related Histone H2A.X Is Mediated by the Protein Phosphatase Eyes Absent. *Journal of Biological Chemistry* 2009, *284*, 16066-16070.

[7] Tran, J.C., L. Zamdborg, D.R. Ahlf, J.E. Lee, et al., Mapping intact protein isoforms in discovery mode using top-down proteomics. *Nature* 2011, *480*, 254-8.

[8] Xie, A., S. Odate, G. Chandramouly, and R.A. Scully, H2AX post-translational modifications in the ionizing radiation response and homologous recombination. *Cell Cycle* 2010, *9*, 3602-3610.

[9] Singh, N., H. Basnet, T.D. Wiltshire, D.H. Mohammad, et al., Dual recognition of phosphoserine and phosphotyrosine in histone variant H2A.X by DNA damage response protein MCPH1. *Proceedings of the National Academy of Sciences* 2012, *109*, 14381-14386.

[10] Brown, J.A.L., J.K. Eykelenboom, and N.F. Lowndes, Co-mutation of histone H2AX S139A with Y142A rescues Y142A-induced ionising radiation sensitivity. *FEBS Open Bio* 2012, *2*, 313-317.
[11] Luger, K., T.J. Rechsteiner, A.J. Flaus, M.M.Y. Waye, et al., Characterization of nucleosome core particles containing histone proteins made in bacteria1. *Journal of Molecular Biology* 1997, *272*, 301-311.
[12] Sie, L., S. Loong, and E.K. Tan, Utility of lymphoblastoid cell lines. *Journal of Neuroscience Research* 2009, *87*, 1953-1959.
[13] Maile, T., A. Izrael-Tomasevic, T. Cheung, G. Guler, et al., Mass Spectrometric Quantification of Histone Posttranslational Modifications by a Hybrid Chemical Labeling Method. *Molecular & Cellular Proteomics* 2015, *14*, 1148-58.
[14] Matheron, L., H. van den Toorn, A.J.R. Heck, and S. Mohammed, Characterization of Biases in Phosphopeptide Enrichment by Ti4+-Immobilized Metal Affinity Chromatography and TiO2 Using a Massive Synthetic Library and Human Cell Digests. *Analytical Chemistry* 2014, *86*, 8312-8320.
[15] Sherrod, S.D., M.V. Myers, M. Li, J.S. Myers, et al., Label-Free Quantitation of Protein Modifications by Pseudo Selected Reaction Monitoring with Internal Reference Peptides. *Journal of Proteome Research* 2012, *11*, 3467-3479.
[16] MacLean, B., D.M. Tomazela, N. Shulman, M. Chambers, et al., Skyline: an open source document editor for creating and analyzing targeted proteomics experiments. *Bioinformatics* 2010, *26*, 966-968.
[17] Zheng, Y., J.D. Tipton, P.M. Thomas, N.L. Kelleher, et al., Site-specific human histone H3 methylation stability: fast K4me3 turnover. *Proteomics* 2014, *14*, 2190-2199.
[18] Olsen, J.V., M. Vermeulen, A. Santamaria, C. Kumar, et al., Quantitative Phosphoproteomics Reveals Widespread Full Phosphorylation Site Occupancy During Mitosis. *Sci. Signal.* 2010, *3*, ra3.
[19] Rigbolt, K.T.G., T.A. Prokhorova, V. Akimov, J. Henningsen, et al., System-Wide Temporal Characterization of the Proteome and Phosphoproteome of Human Embryonic Stem Cell Differentiation. *Sci. Signal.* 2011, *4*, rs3.
[20] Xie, A., A. Hartlerode, M. Stucki, S. Odate, et al., Distinct Roles of Chromatin-Associated Proteins MDC1 and 53BP1 in Mammalian Double-Strand Break Repair. *Molecular Cell* 2007, *28*, 1045-1057.